Fault diagnosis of rolling bearings based on undirected weighted graph

Teng Wang, Guoliang Lu*, Peng Yan
Key Laboratory of High-efficiency and Clean Mechanical Manufacture of MOE, National Demonstration Center for Experimental Mechanical Engineering Education, School of Mechanical Engineering, Shandong University
Jinan 250061, China
wangtengsdu@gmail.com, {luguoliang,yanpeng}@sdu.edu.cn

***Abstract*—One of the main functions of rolling bearing condition monitoring is to diagnosis the type of fault that is occurred during its continuous operations. This paper presents a new method for rolling bearing fault diagnosis based on the graph model. Concretely, through Fourier transform, the periodogram is computed from the condition monitoring (CM) signal and then modeled into an undirected weighted graph. This graph is subsequently fed to K-Nearest Neighbor (KNN) Classifier for fault type diagnosis. In particular, to perform KNN upon graph model, a robust graph distance metric so-called sum of the difference in edge-weight values (SDEWV) is adopted via investigating four candidate metrics existed in the literature. Based on experimental results in the publicly-available database, we demonstrate exciting results of the proposed method in bearing fault diagnosis, indicating its great potentials in real engineering applications.**

***Keywords*—Bearing fault diagnosis, Periodogram, Graph model, K-Nearest Neighbor**

I. INTRODUCTION

Rolling bearings are frequently used in industrial systems but they are also fragile mechanical parts [1]. Therefore, accurate and reliable fault diagnosis for them at an early stage plays an important role in reducing maintenance cost and ensuring the reliability of the monitored machine during its continuous operations [2].

Bearing failures are mostly due to the defects in the outer raceway (OR), inner raceway (IR), or ball [3]. And many researchers (e.g. [3,4]) have demonstrated that the spectrum analysis is a powerful and effective tool to extract failure information from continuous monitoring of bearing condition signals such as vibration and sound. In this line of research, various spectral methods such as frequency spectrum [5], power spectrum [4], envelop spectrum [6], high-order spectrum [7], holospectrum [8] have been widely used to describe/represent the bearing operation condition. In real engineering scenarios, however, the actually acquired condition signals normally involve irregularities and uncertainties in fault status [9]. Thus, it is a common practice in bearing diagnosis to extract high-level features from the resulting spectrum, such as using histogram [10], spectrum kurtosis [11] and empirical cumulative distribution function (ECDF) [3]. These techniques can provide an insight of condition signal in the frequency domain and extract the implicit information related to the bearing health condition. However, the implementation of these techniques on bearing fault diagnosis highly relies on the design and selection of frequency components/features/sub-bands manually. For example, in these practices, the common strategy is extracting the interested frequency components/features/sub-bands which are related to a different type of bearing faults [10]. As this strategy requires the type and exact structure size of the monitored bearing, it is time-consuming and lacks the generalization ability when facing with different applications, especially when this priori knowledge of bearing is unavailable. Meanwhile, although many researchers e.g., [4,12] have shown that the relationships between different frequency components have a discriminative power/capacity when facing with different operation status of rotating machines, most of feature extraction methods fail in mining this information.

Due to the limitation of these methods, this paper proposes a novel bearing fault diagnosis method based on spectrum analysis. In particular, along with the previous work [13], we explore a graph-based modeling strategy that has two main advantages: a) it can represent a class of data from a global view, b) it can describe the relationship between each pair of samples by introducing edge. The flowchart of the proposed method is depicted in Fig. 1. The periodogram is first extracted from the vibration signal of the operating bearing, and then modeled as graph subsequently. To identify the fault type, the graphs are fed to a K-Nearest Neighbor (KNN) classifier combining with a specific graph distance metric called the sum of the difference in edge-weight values (SDEWV).

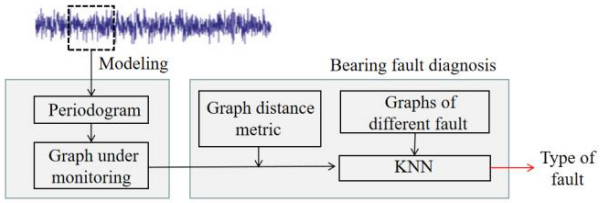

Fig. 1. The diagram of the proposed method.

Main contributions of our study are summarized into two folds:

- Together with graph modeling, a novel spectrum analysis method is developed with the application of

978-1-7281-0329-7/19/$31.00 ©2019 IEEE
DOI 10.1109/PHM-Paris.2019.00013

bearing fault diagnosis. This method does not require any priori knowledge of considered bearing for selection or extraction of spectrum components/features/sub-bands.

- The theoretical interpretation and comprehensive investigation of the proposed method with a public-available database, demonstrating great potential in real applications.

The rest of this paper is organized as follows. In Section II, we give the detail description of this method, and then experiments carried out on a public-available database is introduced in Section III. Finally, Section IV concludes this paper.

II. The Proposed Method

A. Spectrum extraction

As depicted in the literature [3], different type of bearing faults, e.g., OR fault, IR fault, or ball fault, can be reflected in the periodogram that is constructed from monitored condition signals. Let us denote the collected condition signal as $x(n), n \in [0, N-1]$, N is the number of samples, we first give the formulation for periodogram extraction.

The Discrete Fourier Transform (DFT) of $x(n)$ is given as

$$F(k) = \sum_{n=0}^{N-1} x[n]\omega^*[n-M]e^{-j2\pi k\Delta f n} \quad (1)$$

where Δf is frequency interval, $k = 1,2,...,Q$ is the number of frequency contained, $F(k)$ is the output at frequency $k\Delta f$ and the symbol of $*$ denotes the conjugation operation. M is the center of a proper window which can be selected according to the characteristics of processed signals considering the amplitude resolution, frequency resolution, time resolution, etc. Note that a Hanning window with a size of 1×1000 ($1\times T$) is used in this paper. As the choice of best window type is not the purpose of this paper, the comparison of different window types is not reported.

The periodogram of $x(n)$ is then calculated by,

$$P(k) = \frac{1}{T}|F(k)|^2 \quad (2)$$

In Section II-*B*, we will provide the modeling strategy upon the computed $P(k)$.

B. Graph modeling upon periodogram

Although different operation status can be reflected in the periodogram, appropriate modeling/analysis is further required. For this purpose, the acquired periodogram is modeled into graph as it can not only describe the periodogram from a global view but also reveal the relationship between each pair of frequency components by introducing edge.

Generally, a typical graph consists of a set of nodes and edges. And, in this paper, the acquired periodogram $P(k)$ is modeled into undirected weighted graph according to [13] as follows,

a) *Node*: regard each frequency sample $P(k)$ as a node.

b) *Edge*: link each pair of nodes *i* and *j* as an edge L_{ij}.

c) *Weight*: Assign weight d_{ij} to every edge, where d_{ij} is computed as the Euclidean distance between the frequency amplitudes of node *i* and node *j*.

Further, the modeled graph is expressed as an adjacent matric α, i.e., $\alpha = \{d_{ij}\}$, which is symmetric and square. For illustration, Fig. 2 gives the graph modeled from a periodogram $P(k)$, $k \in \{1,2,...,10\}$ and the corresponding adjacent matrix.

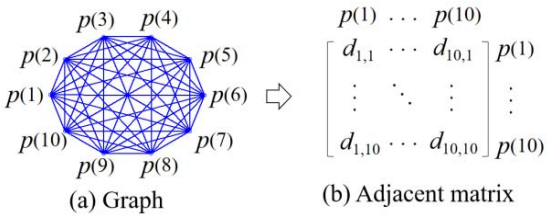

Fig. 2. An example of graph modeling strategy.

C. K-Nearest Neighbor based diagnosis

Since the monitored condition signal has been modeled as graph, the diagnosis of bearing fault can be regarded as a classification task where the training set is composed of graphs each associated with a certain fault label. Fig. 3 provides an example of graphs corresponding to different bearing fault type.

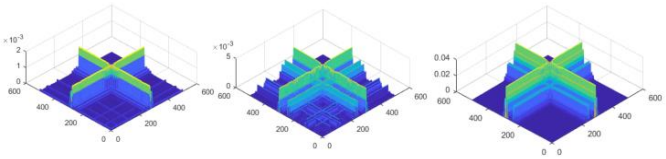

(a) Graph of inner race fault (b) Graph of roller fault (c) Graph of cage fault

Fig. 3. Illustrative example where three type of faults are modeled as graph and the corresponding adjacent matrices are shown in 3D image.

In this research, the widely used lazy learning approach, KNN [14] is adopted for graph classification. Concretely, as illustrated in Fig. 4, distance between the tested graph and training graphs are measured, such that we can obtain *K* nearest neighbors, i.e., the graphs in the training set who have top *K* minimum distance with the tested graph. Subsequently, the label of these neighbors are used to determine the label of the tested graph. In this paper, *K*=3 nearest neighbors are selected to determine the label of the tested graph by voting.

As mentioned in the literature [14], the distance metric plays a critically important role in KNN, reflecting the final classification result dramatically. In this research four candidate graph distance matrices, which are taken/extended from the related literature, are tested. They are,

a) Entropy distance: graph entropy indicates the structural complexity [15] and the corresponding distance metric aims to measure the entropy difference between two graphs as,

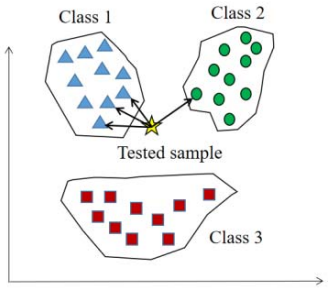

Fig. 4. Illustrative example of KNN where the yellow star represents tested graph. Triangles, squares and circles represent the training graphs in different classes

$$M_e(G,G') = | E(G) - E(G') | \tag{3}$$

where $E(\cdot)$ is the entropy-like measure of the edges and is computed by,

$$E(G) = -\sum_{i=1,j=1}^{i=Q,j=Q} (\overline{d^{i,j}} \times \ln \overline{d^{i,j}}) \tag{4}$$

where

$$\overline{d^{i,j}} = \frac{d^{ij}}{\sum_{i=1,j=1}^{i=Q,j=Q} d^{ij}} \tag{5}$$

b) Spectral distance: according to spectral graph theory, two graphs are similar if their spectrum are close [16]. Thus, spectral distance aims to measure the difference between two graphs in term of their spectrum as,

$$M_s(G,G') = \| S(G) - S(G') \|_2 \tag{6}$$

*w*here ||*|| is L_2*-norm* and *S*(*G*) is the vector consisted with the eigenvalues of graph *G* in strictly descending order.

c) Modality distance: Perron-Frobenius theorem shows that any nonnegative matrix has a nonnegative principal eigenvalue called Perron root and its eigenvector is the so-called perron vector [17]. Modality distance metric aims to measure the difference between two graphs according to their Perron vector as,

$$M_m(G,G') = \| \pi(G) - \pi(G') \|_2 \tag{7}$$

where π（G）is the perron vector of graph *G*.

d) SDEWV distance: SDEWV is defined in [18] and its computational formula is given as,

$$M_{sd} = \sum_{i=1}^{Q} \sum_{j=1}^{Q} \Delta_{i,j} \tag{8}$$

where

$$\Delta_{i,j} = \begin{cases} \dfrac{| d_{i,j} - d'_{i,j} |}{\max\{d_{i,j}, d'_{i,j}\}}, & i \neq j; \\ 0, & i = j. \end{cases} \tag{9}$$

In the following experiment, each graph distance metric above will be embedded in KNN respectively to explore their priority in bearing fault diagnosis.

III. Experiment

A. Experimental setup

The proposed method has been tested on the publicly-available database provided by Case Western Reserve University (CWRU) [19]. The simplified description of the experimental setup is given in Fig. 5, where the induction motor was connected to a dynamometer and the accelerometer was mounted on the drive end of the induction motor for the condition monitoring of a deep groove ball bearing. The bearings were artificial destructed to simulate single point failure using electric spark machining. Specifically, the holes were machined in four different diameters (0.007mm, 0.014mm, 0.021mm, 0.028mm) and in different positions (inner race, outer race, roller, cage), more details about this test platform can be found in [19].

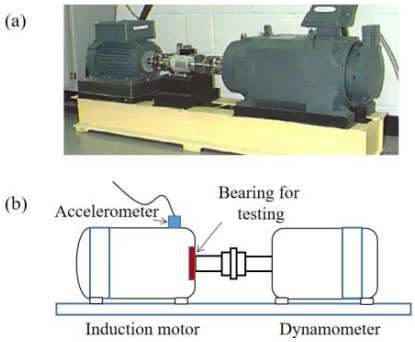

Fig. 5. (a) Experimental setup. (b) Schematic.

In this paper, the faults with 0.007 mm, 0.014 mm, 0.021 mm hole were considered separately as they are three most difficult cases for diagnosis. Table I gives the tested cases and their corresponding labels in the CWRU database.

In summary, 9 classes of faults were considered for diagnosis and the fault signals were collected under four loads (0 hp, 1 hp, 2 hp, 3 hp), thus 36 signals were tested.

In the operation of proposed method, every signal is modeled as a set of graphs by sliding non-overlapping Hanning window as mentioned in Section II. It is worth mentioning that although every signal is modeled into a set of graph, only first 24 graphs in each signal were used. Concretely, the first 12 graphs were stored as training samples

and the following 12 graphs were used for testing using KNN respectively, as a result, 12*36 times of testing were conducted.

TABLE I. TESTED FAULT CLASSES AND THEIR LABELS IN CWRU

Class	Label	Description
1	IROO7	Inner race fault, 0.007mm
2	B007	Ball fault, 0.007mm
3	OR007@6	Outer race fault, 0.007mm
4	IR014	Inner race fault, 0.014mm
5	B014	Ball fault, 0.014mm
6	OR014@6	Outer race, 0.014mm
7	IR021	Inner race, 0.021mm
8	B021	Ball fault, 0.021mm
9	OR021@6	Outer race fault, 0.021mm

B. Diagnosis result

In order to illustrate the operation of proposed diagnosis method, an example is given in Fig. 6 where we randomly selected a kind of bearing fault which belongs to class 2 for testing. Figs. 6 (a)-(d) give the result of KNN in which different graph distance metrics were employed.

From Figs. 6 (a)-(b), we can see that when entropy metric or spectral metric was employed to measure the distance between the tested graph and training graphs, the ground truth (class 2) can not be diagnosed by K-Nearest Neighbors. By contrast, in Figs. 6 (c)-(d), the K-Nearest Neighbors, those are labeled in the red box, all belonged to class 2, which demonstrates the effective of modality distance as well as SDEWV distance in proposed method.

For comprehensive evaluation, Fig. 7 gives the diagnosis accuracy using different graph distance metrics. It can be seen that SDEWV based KNN exhibited a prefect performance in bearing fault diagnosis where all of the fault cases were classified correctly, thus 100% diagnosis accuracy was achieved. However, entropy distance based KNN showed the worst diagnosis accuracy (9.26%), followed with spectral distance based KNN (56.02%) and modality distance based KNN (98.15%). One of the reasons is that all of the entropy, spectral and modality distances require mapping operation; while, this mapping operation destroys the separability of different bearing faults. In other words, it is more difficult to discriminate different fault types in the spaces mapped. In this regard, the SDEWV based KNN is recommended for usage in the proposed framework for bearing fault diagnosis.

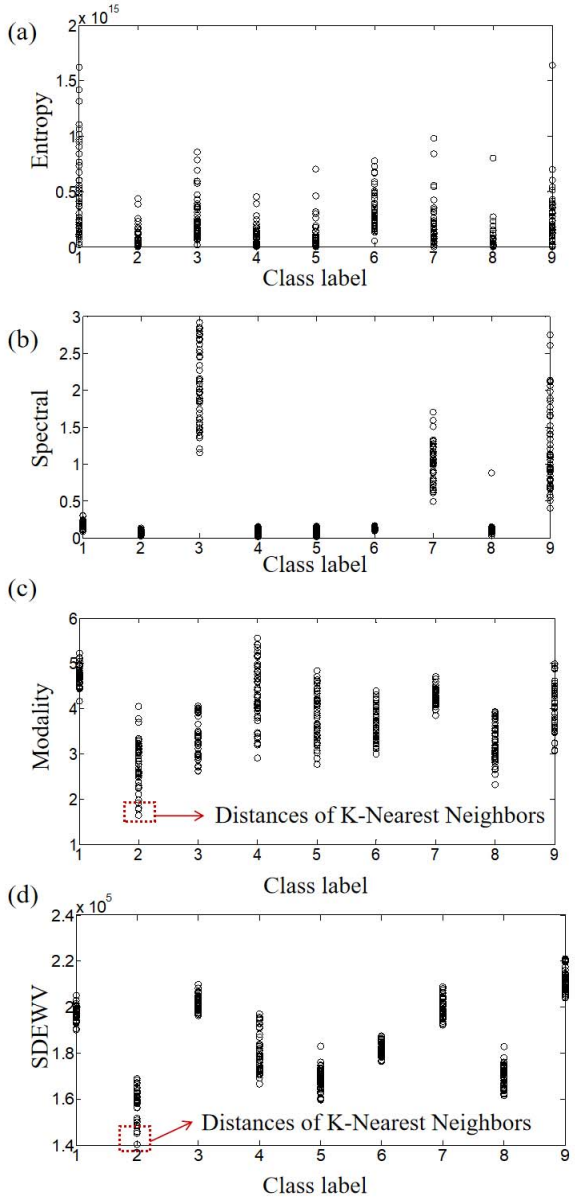

Fig. 6. The result of KNN combining with different graph distance metrics: (a) KNN+Entropy distance; (b) KNN+Spectral distance; (c) KNN+Modality distance; (d) KNN+SDEWV distance.

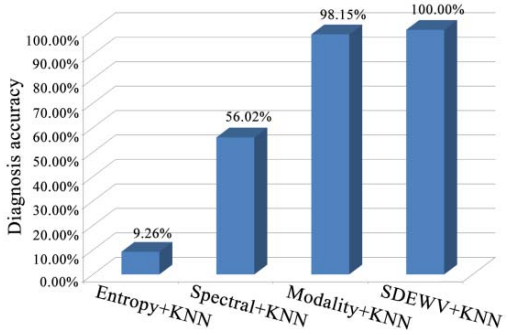

Fig. 7. The result of KNN combining with different graph distance metrics.

IV. Conclusion

In this paper, we have presented a new method for bearing fault diagnosis where the periodogram of the CM signal is modeled as graphs for analysis. Specifically, the K-Nearest Neighbor algorithm was adopted for fault classification.

Meanwhile, in order to find an appropriate graph distance metric for usage, four candidate graph distances taken from the literature were tested in this paper. As a result, the metric called SDEWV shown excellent performance in bearing fault diagnosis, thus is recommended for usage. Compared with the existed method in this area, the proposed method aims to describe the spectrum from a globe view, thus does not need the priori knowledge of bearing type and structure for spectrum components/features selection and extraction.

In the future, we will further extend this modeling strategy to anomaly detection during the continuous operation of bearing.

References

[1] P. O. Donnell, C. Heising, C. Singh, and S. J. Wells, "Report of large motor reliability survey of industrial and commercial installatons: part I," IEEE Trans. Ind. Appl., vol. 23, no. 4, pp. 153-158, 1987.

[2] Z. Gao, C. Cecati, and S. X. Ding, "A survey of fault diagnosis and fault-tolerant techniques: part I: fault diagnosis with model-based and signal-based approaches," IEEE Trans. Ind. Electron., vol. 62, no. 6, pp. 3757-3767, 2015.

[3] L. Ciabattoni, F. Ferracuti, A. Freddi, and A. Monteriu, "Statistical spectral analysis for fault diagnosis of rotating machines," IEEE Trans. Ind. Electron., vol. 65, no. 5, pp. 4301-4310, 2018.

[4] B. Liang, S. D. Iwnicki, Y. Zhao, "Application of power spectrum, cepstrum, higher order spectrum and neural network analyses for induction motor fault diagnosis," Mech. Syst. Signal Process., vol. 39, no. 1-2, pp. 342-360, 2013.

[5] E. H. E. Bouchikhi, V. Choqueuse, M. E. H. Benbouzid, "Current frequency spectral subtraction and its contribution to induction machines' Bearings Condition Monitoring," IEEE Trans. Energy Convers., vol. 28, no. 1, pp. 135-144, 2013.

[6] D. Abboud, J. Antoni, S. Sieg-Zieba, and M. Eltabach, "Envelope analysis of rotating machine vibrations in variable speed conditions: a comprehensive treatment," Mech. Syst. Signal Process., vol. 84, pp. 200-226, 2017.

[7] A. C. Mccormick, and A. K. Nandi, "Bispectral and trispectral features for machine condition diagnosis," IEE P-Vis. Image. Sign., vol. 146, no. 5, pp.229-234, 1999.

[8] L. Qu, X. Liu, G. Peyronne, Y. Chen, "The holospectrum: a new method for rotor surveillance and diagnosis," Mech. Syst. Signal Process., vol. 3, no. 3, pp. 255-267, 2003.

[9] M. S. Kan, A. C. C. Tan, and J. Mathew, "A review on prognostic techniques for non-stationary and non-linear rotating systems," Mech. Syst. Signal Process., vol. 62-63, pp. 1-1, 2017.

[10] Diego FernándezFrancos, David MartínezRego, Fontenlaromero O. , et al. "Automatic bearing fault diagnosis based on one-class ν -SVM," Comput. Ind. Eng., vol. 64, no. 1, pp. 357-365, 2013.

[11] N. Sawalhi, R. B. Randall, H. Endo, "The enhancement of fault detection and diagnosis in rolling element bearings using minimum entropy deconvolution combined with spectral kurtosis," Mech. Syst. Signal Process., vol. 21, no. 6, pp. 2616-2633, 2007.

[12] G. Betta, C. Liguori, A. Paolillo, and A. Pietrosanto, "A DSP-based FFT-analyzer for the fault diagnosis of rotating machine based on vibration analysis." IEEE Trans. Instrum. Meas., vol. 1, pp. 572-577, 2001.

[13] G. Lu, J. Liu, P. Yan, "Graph-based structural change detection for rotating machinery monitoring," Mech. Syst. Signal Process, vol. 99, pp. 73-82, 2018.

[14] T. M. Cover, "Nearest neighbor pattern classification," IEEE Trans. Inf. Theory, vol. 13, no. 1, pp. 21-27, 1967.

[15] E. Trucco, "A note on the information content of graphs," Bulletin of Mathematical Biophysics, vol. 18, no. 2, pp. 129-135, 1956.

[16] K. Beyer. J. Goldstein, R. Ramakrishnan, and U. Shaft, "When is nearest neighbor meaningful?" in Proc. Int. Conf. Data Theo., vol. 1540, pp. 271-235, 1999.

[17] A. Berman, and R. J. Plemmons, "Nonnegative matrices in the mathematical sciences." New York: Academic Press. 1979.

[18] T. Wang, G. Lu, J. Liu and P. Yan, "Graph-based change detection for condition monitoring of rotating machines: Techniques for graph similarity," IEEE Trans. Reliab., pp. 1-16, 2018.

[19] W. A. Smith and R. B. Randall, "Rolling element bearing diagnosis using the Case University data: A benchmark study," Mech, Syst. Signal Process., vol. 64, pp. 100-131, 2015.